Environmental Science and Ecotechnology 22 (2024) 100442

Contents lists available at ScienceDirect

Environmental Science and Ecotechnology

journal homepage: www.journals.elsevier.com/environmental-science-and-ecotechnology/

Original Research

65% cover is the sustainable vegetation threshold on the Loess Plateau

Yi-ping Chen [a, *], Kai-bo Wang [a], Bo-jie Fu [b], Yan-fen Wang [c], Han-wen Tian [a, c], Yi Wang [a], Yi Zhang [a]

[a] State Key Laboratory of Loess Science, Institute of Earth Environment, Chinese Academy of Sciences, 700061, Xi'an, China
[b] Research Center for Eco-environmental Sciences, Chinese Academy of Sciences, 100085, Beijing, China
[c] University of Chinese Academy of Sciences, 100049, Beijing, China

ARTICLE INFO

Article history:
Received 2 September 2023
Received in revised form
13 June 2024
Accepted 13 June 2024

Keywords:
Climate change
Loss plateau
Vegetation change
Sustainable development
Yellow River

ABSTRACT

Global temperatures will continue to increase in the future. The ~640,000-km^2 Loess Plateau (LP) is a typical arid and semi-arid region in China. Similar regions cover ~41% of the Earth, and its soils are some of the most severely eroded anywhere in the world. It is very important to understand the vegetation change and its ecological threshold under climate change on the LP for the sustainable development in the Yellow River Basin. However, little is known about how vegetation on the LP will respond to climate change and what is the sustainable threshold level of vegetation cover on the LP. Here we show that the temperature on the LP has risen 0.27 °C per decade over the past 50 years, a rate that is 30% higher than the average warming rate across China. During historical times, vegetation change was regulated by environmental factors and anthropogenic activities. Vegetation coverage was about 53% on the LP from the Xia Dynasty to the Spring and Autumn and Warring States period. Over the past 70 years, however, the environment has gradually improved and the vegetation cover had increased to ~65% by 2021. We forecast future changes of vegetation cover on the LP in 2030s, in 2050s and in 2070s using SDM (Species Distribution Model) under Low-emission scenarios, Medium-emission scenarios and High-emission scenarios. An average value of vegetation cover under the three emission scenarios will be 64.67%, 62.70% and 61.47%, respectively. According to the historical record and SDM forecasts, the threshold level of vegetation cover on the LP is estimated to be 53–65%. Currently, vegetation cover on the LP has increased to the upper limit of the threshold value (~65%). We conclude that the risk of ecosystem collapse on the LP will increase with further temperature increases once the vegetated area and density exceed the threshold value. It is urgent to adopt sustainable strategies such as stopping expanding vegetation area and scientifically optimizing the vegetation structure on the LP to improve the ecological sustainability of the Yellow River Basin.

1. Introduction

Launched in 1999 by the Chinese government, the Grain for Green (GFG) project has become the largest ecological restoration initiative [1,2]. The central government of China has invested over RMB 500 billion (~USD 73 billion) in this project, and 33 million hectares of farmland have been converted into forests and grass (http://www.forestry.gov.cn/). Forest coverage countrywide increased from 16.6% in 1998 to 24.02% in 2021 (http://www.forestry.gov.cn/). The greatest increase in vegetation coverage occurred on the Loess Plateau, from 31.6% in 1999 to 59.6% in 2013 [3]. With the continuous progress of the GFG project, China has become the largest contributor to global ecological restoration, contributing ~25% of total global "greening" [4].

Covering approximately 640,000 km^2, the Loess Plateau in China is characterized by semi-humid and semi-arid conditions. Regions with similar conditions comprise about 41% of Earth's total land area and feature some of the most severely eroded soils globally. Climatic warming, ongoing during the GFG project, is expected to continue in the foreseeable future [5,6]. An increase in temperature-induced drought episodes over half of the global land surface between 2071 and 2100 [7]. Increasing temperature-induced intensification of dry seasons has been observed over the last century [8], leading to hotter droughts. In this regard, rising

* Corresponding author.
E-mail address: lifesci@ieecas.cn (Y.-p. Chen).

https://doi.org/10.1016/j.ese.2024.100442

temperatures have also led to a substantial increase in the occurrence of warm-season droughts in Asia during recent years [9]. Between 1909 and 2011, the average land temperature increase rate has been higher than the global average, reaching 0.9–1.5 °C. However, significant regional variations exist in domestic climate change [5,6]. Limited research has been published on climate change and its impact on vegetation dynamics on the Loess Plateau, considering expected future warming.

The global climate models (GCMs) may accurately predict global climate change and variability ratio, integrating multiple earth systems such as the atmosphere, ocean, land surface, and sea ice. They can provide information on the impact of climate change on the global and regional levels and assist in analyzing adaptation strategies and vulnerability assessments [10]. The Phase 6 coupled model intercomparison project (CMIP6) of the climate model has comprehensively considered the socio-economic path and representative concentration path (RCP) scenarios, which have been widely used to quantitatively describe the challenges humans will face under different future climate scenarios [11]. Assessing and predicting the impact of climate warming on vegetation growth is a critical task in ecology. Species distribution models (SDMs) are classical models [12] widely used to assess and predict the impact of climatic changes on species number and distribution [13–16].

To maintain the sustainability of the GFG project and provide scientific strategies for vegetation management under climate change on the Loess Plateau. Based on existing distribution data and future climate environment variables, principal component analysis, correlation coefficient contribution method, and screening methods are used to extract highly correlated environmental variables. Here we analyzed the trends in temperature, precipitation, evaporation, humidity, and wind speed, and then analyzed the relationship and effect on vegetation cover, finally forecasted the future vegetation change (the 2030s, 2050s, and 2070s) by using the model/algorithm for providing some advice on sustainable development in the Yellow River Basin.

2. Methods and materials

2.1. Data sources

Relative humidity, wind speed, precipitation, evaporation, and temperature were obtained from the National Meteorological Center and National Earth System Science Data Center (http://data.cma.cn/data/weatherBk.html) (http://loess.geodata.cn). Remotely sensed satellite data (SPOT/VGT ten-day synthetic NDVI data) were obtained from the Western China Environmental and Ecological Science Data Center (http://westdc.westgis.ac.cn). Select BCC_CSM2 (Beijing Climate Center) suitable for China for the next three climate scenarios. The medium-resolution version of the Beijing climate center climate system model, version 2, is sourced from the National Aeronautics and Space Administration (NASA) Earth exchange global daily downscale projections (NEX-GDDP-CMIP6) data. We have calculated the annual temperature and precipitation data from the original data as mean annual temperature (MAT), annual accumulated temperature (AAT) $\geq$ 0 °C, and mean annual precipitation (MAP) for three time periods of 2030, 2050, and 2070s. The climate data for the base year (1990–2020) is sourced from the climatic research unit (CRU) time series (TS) version 4.05, with a spatial resolution of 0.5°. Sediment data were obtained from the Yellow River Water Conservancy Commission (http://www.yrcc.gov.cn/). Vegetation data (1982–1999) were obtained from Gao et al. [17].

2.2. Maximum value composites

Remotely sensed satellite data (January 1998–December 2021) were pre-processed to correct atmospheric and radiation effects and corrected for geometry before generating NDVI at a temporal resolution of ten days. Subsequently, the maximum NDVI values from each ten-day interval were employed to document large-scale changes in vegetation cover [18].

Maximum value composites (MVC) are the predominant method for calculating vegetation coverage [19]. The principle is to use the maximum monthly NDVI to eliminate partial interference of clouds, particles, shadows, and solar height angles in the atmosphere. Maximum NDVI values for April through October were obtained by the MVC method, renowned for its efficacy in reducing the influence of clouds, aerosols, cloud shadows, sensor observation angles, and solar altitude angles in the atmosphere. The specific formula is as follows:

$$\mathrm{NDVI}_{\max,i} = \max(\mathrm{NDVI}_1\ ,\ \mathrm{NDVI}_2\ ,\ \mathrm{NDVI}_3\ ,\ \mathrm{NDVI}_4) \quad (1)$$

where $\mathrm{NDVI}_{\max,i}$ represents the maximum monthly NDVI value; i represents the month, ranging from 4 to 10; NDVI_1 , NDVI_2 , NDVI_3 , NDVI_4 represents the NDVI values of the preprocessed original images synthesized within eight days of the corresponding month.

2.3. The pixel dichotomy model

Vegetation cover and NDVI are strongly linearly correlated. By establishing the relationship between them, vegetation cover can be estimated from NDVI; the pixel dichotomy model is used to estimate vegetation cover [20]. Assuming that the NDVI values of each pixel can be synthesized from both vegetation and soil, the formula is as follows:

$$\mathrm{NDVI} = NDVI_{\mathrm{v}} C_i + NDVI_{\mathrm{s}}(1 - C_i) \quad (2)$$

where $NDVI_{\mathrm{v}}$ is the NDVI value of the vegetation cover part, $NDVI_{\mathrm{s}}$ is the NDVI value of the soil part, and C_i is the vegetation cover degree. C_i can be estimated as:

$$C_i = \frac{\mathrm{NDVI} - NDVI_{\mathrm{s}}}{NDVI_{\mathrm{v}} - NDVI_{\mathrm{s}}} \quad (3)$$

The pixel dichotomy model is widely used to calculate vegetation coverage because of its insensitivity to image radiation correction [21]. However, the model also has some defects. NDVI not only reflects vegetation cover but also reflects land-cover type and leaf area index (LAI). For unvegetated pixels, $NDVI_{\mathrm{s}}$ should be close to 0 and not change over time. But because of atmospheric conditions, surface humidity, solar lighting conditions, etc., $NDVI_{\mathrm{s}}$ is not fixed but vary from −0.1 to +0.2. For pure vegetation images, the type of vegetation and its composition, the spatial distribution of vegetation, and the seasonal variation of vegetation growth all cause spatiotemporal variation in $NDVI_{\mathrm{v}}$. At present, there are many ways to estimate $NDVI_{\mathrm{v}}$ and $NDVI_{\mathrm{s}}$. Some researchers have set $NDVI_{\mathrm{v}}$ and $NDVI_{\mathrm{s}}$ for each vegetation type as fixed values, calculate C_i based on previous research experience. Using the grayscale distribution of NDVI across the whole image, the maximum and minimum grayscale values can be taken to represented $NDVI_{\mathrm{v}}$ and $NDVI_{\mathrm{s}}$ respectively, with a confidence level of 0.5% [22].

In the actual calculation process, the maximum and minimum values of vegetation NDVI in the growing season are assumed to be $NDVI_{\mathrm{v}}$ and $NDVI_{\mathrm{s}}$, vegetation cover is estimated as:

$$C_i = \frac{\mathrm{NDVI} - NDVI_{\min}}{NDVI_{\max} - NDVI_{\min}} \quad (4)$$

where $NDVI_{\min}$ and $NDVI_{\max}$ are the maximum and minimum values of vegetation NDVI for the entire growing season, respectively.

2.4. Classification of vegetation coverage

To characterize vegetation cover and its temporal change, point estimates of cover are needed. However, there is no uniform way to measure vegetation cover. Therefore, based on previous research results [23,24] and direct observations on the Loess Plateau, we divided our estimates of vegetation cover into eight percentiles: 0–20%, 20–30%, 30–40%, 40–50%, 50–60%, 60–70%, 70–80%, and 80–100%.

2.5. Estimation of changes in vegetation cover

We calculated changes in vegetation cover between successive years using ArcGIS version 10.2 and its built-in spatial interpolation (data has been described in the data source section).

2.6. Species distribution models

Species distribution models (SDMs) use principal component analysis, correlation coefficient method, and other variable screening methods to extract weakly correlated environmental variables based on the existing distribution data and environmental variables of species. These models use models or algorithms to infer the niche requirements of species and evaluate or predict their suitability for existence. Using SDMs enables the assessment of habitat suitability and yields predictions beyond the capabilities of alternative models. By comparing ecological conditions where species are present, SDMs determine the suitability of various locations within the study area for species survival and predict potential future distribution areas.

2.7. Climate tendency method

The change-slope method adopts ordinary linear regression analysis to analyze each grid point's trend change. This paper uses this method [25] to simulate the change rate of vegetation greenness (Greenness Rate of Change or GRC). GRC is the slope of the linear regression equation of the minimum power of the annual change of the seasonally integrated normalized difference vegetation index (SINDVI). This method is used here to simulate the variation trend of maximized NDVI over the years:

$$\theta_{\mathrm{slope}} = \frac{n \times \sum_{i=1}^{n} i \times M_{\mathrm{NDVI},1} - \sum_{i=1}^{n} i \sum_{i=1}^{n} M_{\mathrm{NDVI},i}}{n \times \sum_{i=1}^{n} i^2 - \left(\sum_{i=1}^{n} i\right)^2} \quad (5)$$

where variable i is the annual number from 1 to 10; $M_{\mathrm{NDVI},i}$ represents the maximum NDVI value in year i. The change trend chart reflects the change trend of NDVI in China over a ten-year time series. The trend line of an image point is the overall trend of the maximum NDVI value of the image point over ten years simulated by unary linear regression. θ_{slope} is the slope of this trend line. The trend line is not a simple last-year to first-year line. $\theta_{\mathrm{slope}} > 0$ indicates that the changing trend of NDVI in seven years is increasing; the opposite is a decrease.

We used a sliding t-test to assess whether the difference between two groups of sample averages is significantly different from zero (no temporal change). For a time series x with n observations, the time point is artificially set at a certain point, the samples of the two sub-sequences before and after the base point x_1 and x_2 are n_1 and n_2, the two sub-sequences are $\overline{x_1}$ and x_2, and the variances are S_1^2 and S_2^2, respectively. The statistic is defined using equations (6) and (7):

$$s = \sqrt{\frac{n_1 s_1^2 + n_2 s_2^2}{n_1 + n_2 - 2}} \quad (6)$$

$$t = \frac{\overline{x_1} - \overline{x_2}}{s \cdot \sqrt{\frac{1}{n_1} + \frac{1}{n_2}}} \quad (7)$$

2.8. Soil collection and analysis

Soil samples were collected at a depth of 30 cm in the center of the Loess Plateau at different sites (110°31′–107°41′ E, 35°21′–37°31′ N) in May 2019. Three sites with similar conditions and land-use patterns were selected: (1) slope farmland (SFL) planted with potato (*Solanum tuberosum* L.) or Maize (*Zea mays* L.) for 20 years; (2) forestland (RFL), returning farmland to locust (*Robinia pseudoacacia* L.) for 20 years; and (3) grassland (RGL), resulting from slope farmland that had been abandoned for 20 years. Five points were randomly selected in each site, and five 30-cm deep soil cores were taken at each sampling point. We thoroughly mixed the five-point samples into one aggregated sample, then put in plastic bags for analysis. Soil samples were dried at 105 °C to constant weight, and soil water content (SWC) was measured. SWC (%) was calculated according to formula [(wet soil weight − dry soil weight) / dry soil weight] × 100.

All statistical analyses were done using the SPSS 20.0 software (IBM SPSS Statistics, IBM Corp., USA); the significance level was set at $P < 0.05$ level. Differences among SFL, RGL, and RFL were compared using one-way ANOVA followed by Tukey post-hoc tests.

3. Results and discussion

3.1. Climatic change on the loess plateau

Using 1986–2005 as the current benchmark, the average global surface temperature increase from 2016 to 2035 is forecast to be 0.3–0.7 °C and up to 4.8 °C by the end of the 21st century [26,27]. These increases exceed the 2 °C warming thresholds that governments worldwide have pledged to maintain and will lead to new ecological issues. Such issues are likely to be especially severe in the world's ~6.1 × 10^7 km^2 semi-humid and semi-arid regions, about 41% of the Earth's terrestrial surface [28,29]. Measured air temperature on the Loess Plateau has risen steadily over the past 50 years (Fig. 1). The average rate of warming on the Loess Plateau was 0.27 °C per decade, more than double the global average (0.12 °C per decade) and 30% higher than the average warming rate across China (0.19 °C per decade). Relative to the 1968–1977 decadal average (Fig. 1), average air temperature on the Loess Plateau increased by 0.46 °C from 1978 to 1987, 0.50 °C from 1988 to 1997, 0.30 °C from 1998 to 2007, and 0.70 °C from 2008 to 2017. Precipitation (Fig. 2a), humidity (Fig. 2b), and evaporation (Fig. 2c) generally also have increased, albeit at different rates, over the past 40 years, whereas wind speed has slowed slightly (Fig. 2d).

The large increase in evaporation, unaccompanied by a

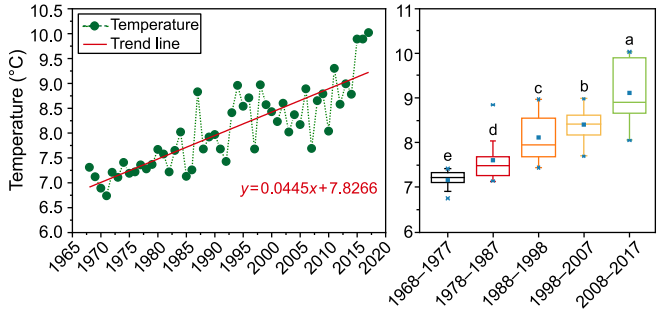

Fig. 1. Temperature trend from 1968 to 2017 on the Loess Plateau. The left panel illustrates the annualized time series, and the right panel shows decadal average air temperatures relative to the 1985–2005 benchmark. Boxes in the right panel with different letters above them are significantly different from one another ($P < 0.05$).

comparable increase in rainfall, will result in soil drought on the Loess Plateau. Previous research has forecast that the warming and drying trends on the Loess Plateau will continue through 2100 [30,31], and the trends will be accompanied on the Loess Plateau by extreme rainfall events, longer heatwaves, and prolonged drought [30,31]. These trends will limit the prospects for consolidating the achievements of the GFG project and reduce the likelihood of successful sustainable development of the Yellow River Basin.

3.2. Vegetation change on the loess plateau

Vegetation is among the most important components of terrestrial ecosystems, undertaking important ecological functions such as soil and water conservation, climate and water regulation, and so on [32,33]. Vegetation dynamics are affected not only by environmental factors but also by past and current human activities. In historical times, vegetation cover on the Loess Plateau was dramatically reduced by human actions (Fig. 3a). From the Xia Dynasty to the Spring and Autumn and Warring States period (2070–221 BCE), vegetation cover was near its historical maximum of ~53% on the Loess Plateau [34]. Vegetation cover decreased to 45% during the Qin and Han Dynasties (221 BCE–202 CE). During the frequent dynastic changes in the 360 years from the end of the Han Dynasty to the period of the North and South Dynasties, land-use changes further reduced vegetation cover to ~40% [35]. This trend continued during the Sui and Tang Dynasties (581–907 CE), when vegetation cover decreased to ~35%. From the end of the Tang dynasty to the founding of the People's Republic of China (907–1949 CE), land use and conflicts on the Loess Plateau reduced vegetation cover to its historic low of ~6% (Fig. 3a) [36].

Over 70 years, vegetation has returned overwhelmingly on the Loess Plateau. Vegetation cover increased by ~5% from 1981 to 1999 (light yellow section in Fig. 3a) and then much more rapidly after the implementation of the GFG project (Fig. 3a). In absolute terms, the vegetation cover in 2012 (Fig. 3a) was comparable to the historical maximum recorded during the Xia Dynasty. Since 2012, vegetation cover on the loess plateau has increased further, reaching ~64.23% in 2021, which was a 0.75% decrease compared with 2019 (Fig. 3b). However, these changes were not spatially uniform (Fig. 3c and d). From 1999 to 2012, vegetation cover increased within the central trunk of the Yellow River basin while it decreased to the east (in eastern Gansu Province) and west (Fenwei Plain), the latter resulted partly from agricultural activity (Fig. 3c). From 2012 to 2021, loss of vegetation was concentrated in two regions: a rapid decline in eastern Gansu province and on the border between Shaanxi and Gansu provinces; and slower declines in the tributary basins of the Yellow River. In other areas, vegetation cover increased steadily in most areas of the eastern loess Plateau (Fig. 3d).

From southeast to northwest, the Loess Plateau has four vegetation zones (Fig. S1) [37]. These, in turn, are the temperate, semi-humid, broad-leaved, deciduous forest zone (SHFZ); the temperate, arid forest zone (TAFZ); the temperate, semi-arid steppe zone (TSSZ); and the temperate arid steppe zone (TASZ). Vegetation cover in all four vegetation belts increased from 1999 to 2021

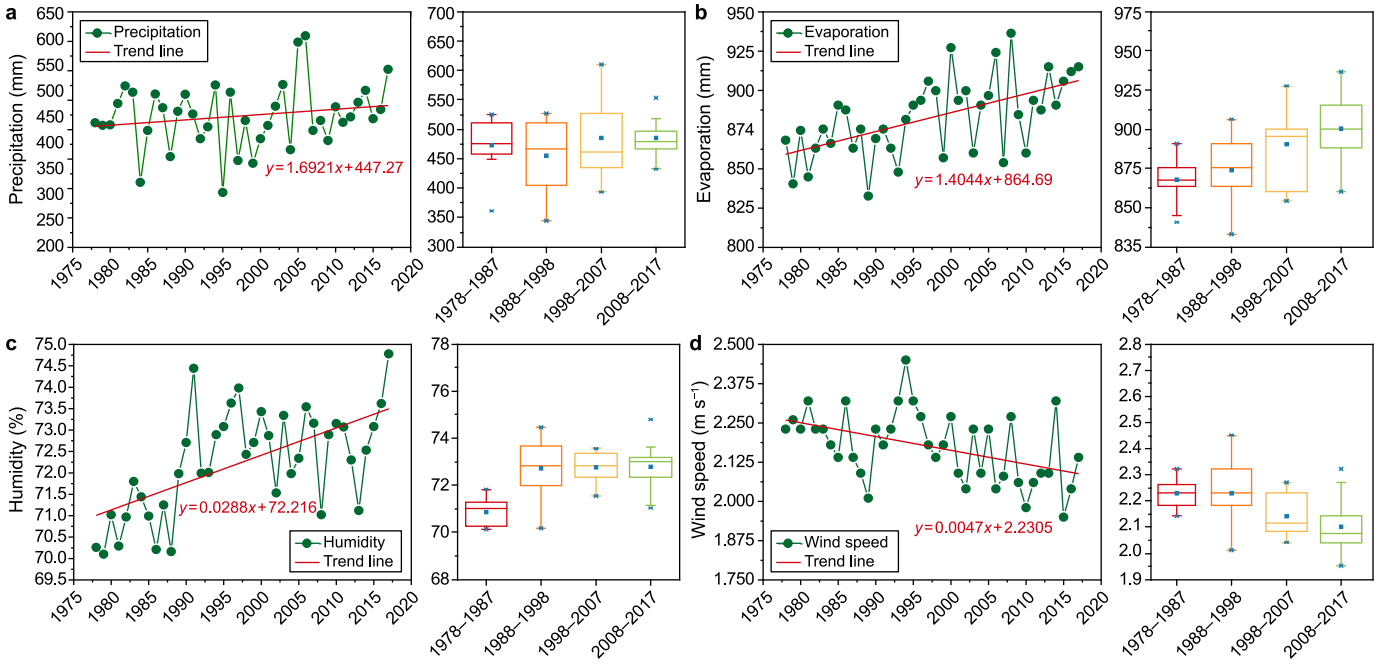

Fig. 2. Changes in precipitation (**a**), evaporation (**b**), humidity (**c**), and wind speed (**d**) from 1978 to 2017 on China's Loess Plateau. The left panels show the time series; the right panels illustrate decadal average changes.

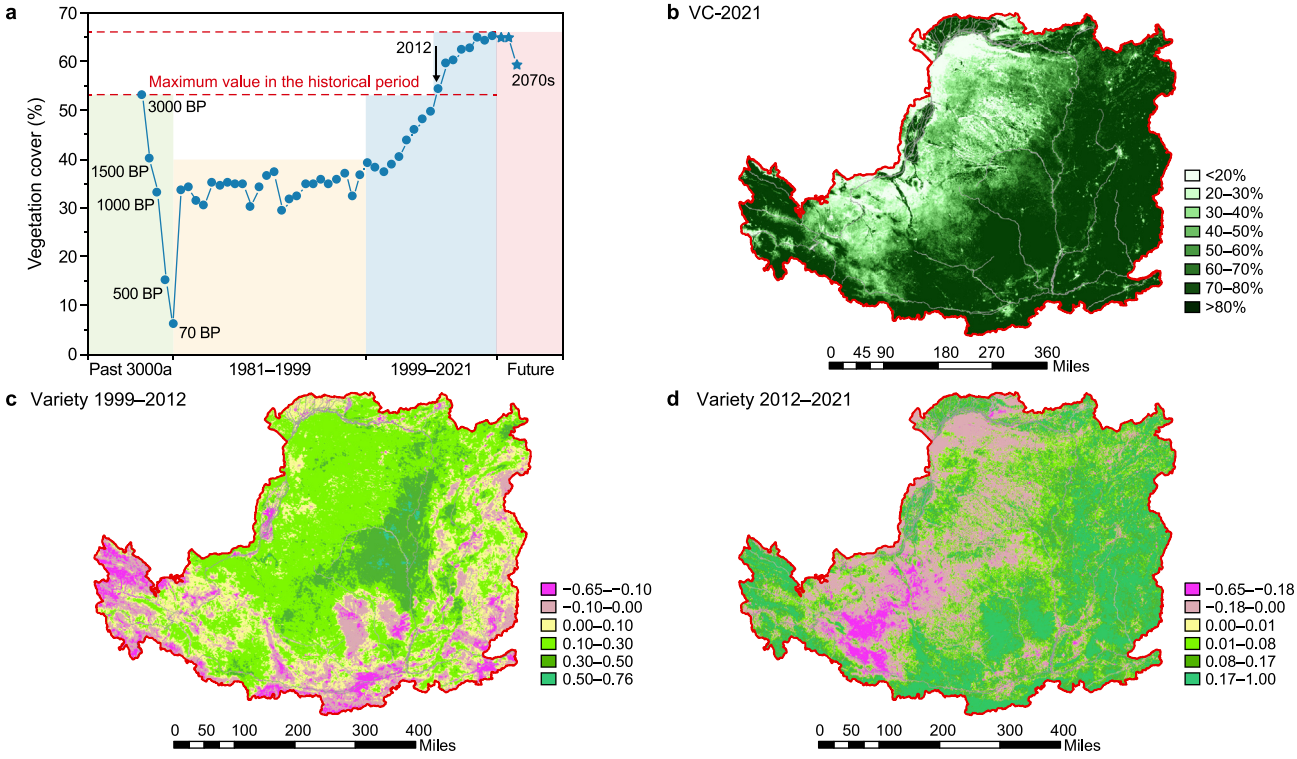

Fig. 3. **a**, Trends in vegetation coverage in the historical record. **b**, Total vegetation cover in 2021. **c**–**d**, spatial variation in vegetation change in 1999–2012 (**c**) and 2012–2021 (**d**) on China's Loess Plateau.

(Fig. 4a–d), with the vegetation cover increase of TAFZ (1.2% yr^{-1}) > TSFZ (1.1% yr^{-1}) > TSSZ (0.9% yr^{-1}) > TASZ (0.4% yr^{-1}). However, the vegetation cover has shown a tendency to decline since 2019.

The nature and direction of future changes remain uncertain. Predictions play an important role in alerting scientists and decision-makers to potential future risks, providing a means to bolster the attribution of biological changes to climate change, and supporting the development of proactive strategies to reduce climate change impacts on biodiversity [38,39]. The forecast results

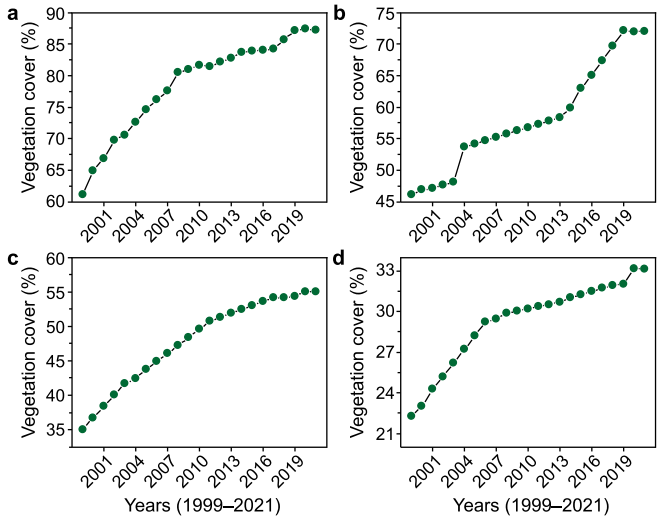

Fig. 4. Vegetation cover from 1999 to 2021 in the four different vegetation zones (Fig. S1) on the Loess Plateau. **a**, Temperate, semi-humid, broad-leaved, deciduous forest zone (TSFZ). **b**, Temperate arid forest zone (TAFZ). **c**, Temperate semi-arid steppe zone (TSSZ). **d**, Temperate arid steppe zone (TASZ).

of vegetation cover are 66% (Fig. 5a), 65% (Figs. 5b), and 64% (Fig. 5c) in the 2030s, 2050s, and 2070s on the Loess Plateau under the low-emission scenarios, respectively. Forecasted vegetation cover is 68% (Figs. 5d), 64% (Fig. 5e), and 63% (Fig. 5f) with the intermediate-emission scenario and 60% (Figs. 5g), 59% (Fig. 5h), 58% (Fig. 5i) with the high-emission scenario.

The overall average forecasted values of the three emission scenarios for the three focal decades ($P > 0.05$) are 65%, 63%, and 62% (Fig. S2), all of which are lower than the vegetation cover observed in 2019. These results suggest that overall vegetation cover may have peaked on the Loess Plateau and that the future sustainability of the region does not require more vegetation cover. However, the different vegetation zones are forecast to respond differently to warming and increased CO_2, decreasing gradually from the 2030s to the 2070s in the SHFZ (Fig. 6a), TAFZ (Fig. 6b), and TSSZ (Fig. 6c), of which insignificant decreasing will be between 2030s and 2050s, between 2050s and 2070s except for TSSZ. However, significant increases ($P < 0.05$) during the same time in the TASZ from the 2030s–2070s (Fig. 6d). These differences necessitate different management policies for the different vegetation zones on the Loess Plateau.

3.3. *Vegetation effects on sustainable development in the Yellow River Basin*

Under the background of global warming, the increasing vegetation coverage and unreasonable vegetation structure have led to the aggravation of regional water resources consumption the Loess Plateau. As a typical semi-humid and semi-arid region. The Loess Plateau has experienced a rapid increase in vegetation coverage and a continuous rise in temperature in the past few decades, which not only improves the regional environment, but also brings soil desiccation.

Historical data illustrate that flooding of the Yellow River has

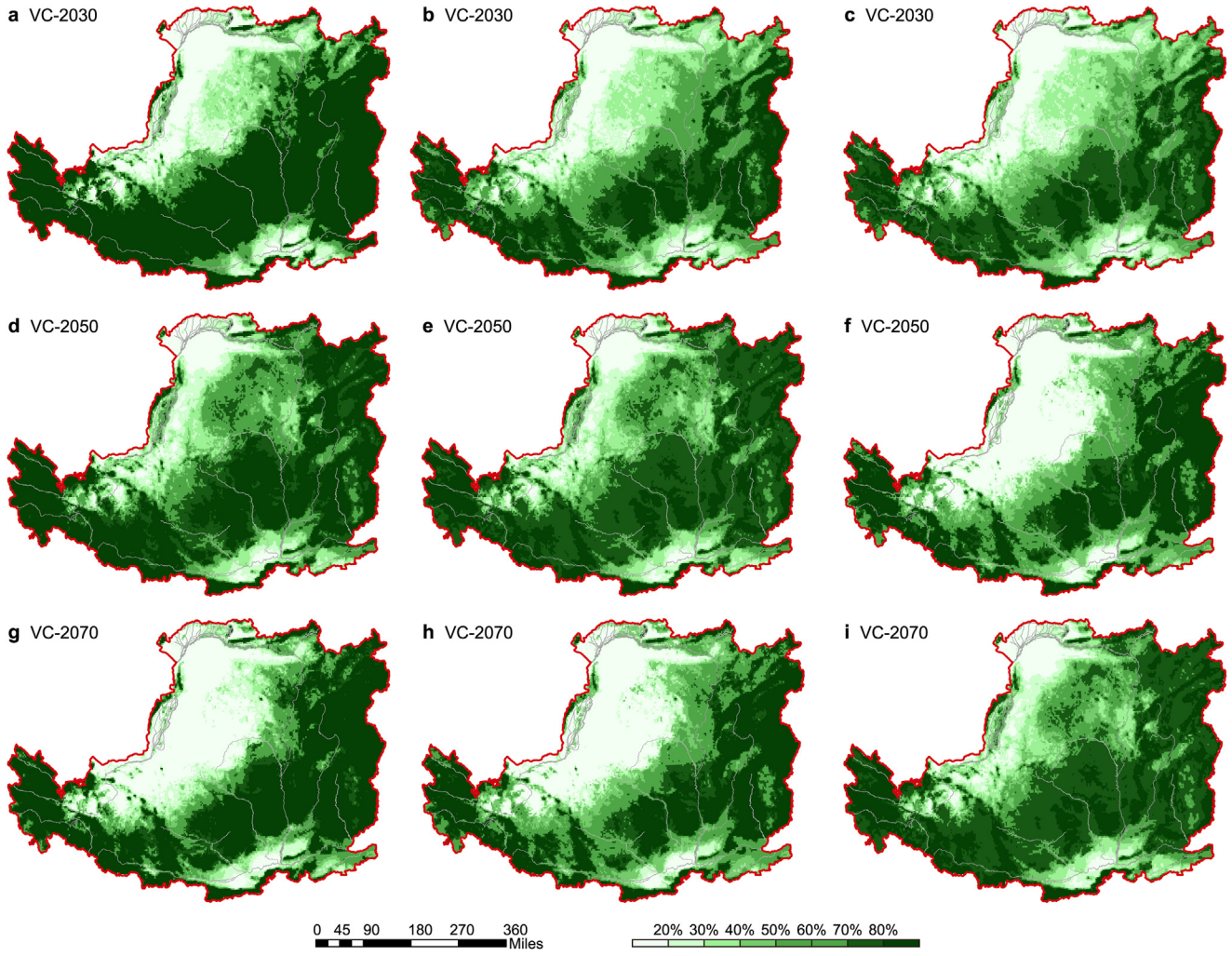

Fig. 5. Vegetation cover (VC) on China's Loess Plateau in the 2030s (**a**–**c**), 2050s (**d**–**f**), and 2070s (**g**–**i**) forecast using species distribution models (SDMs) run under low (**a**, **d**, **g**), intermediate (**b**, **e**, **h**), and high (**c**, **f**, **i**) emission scenarios.

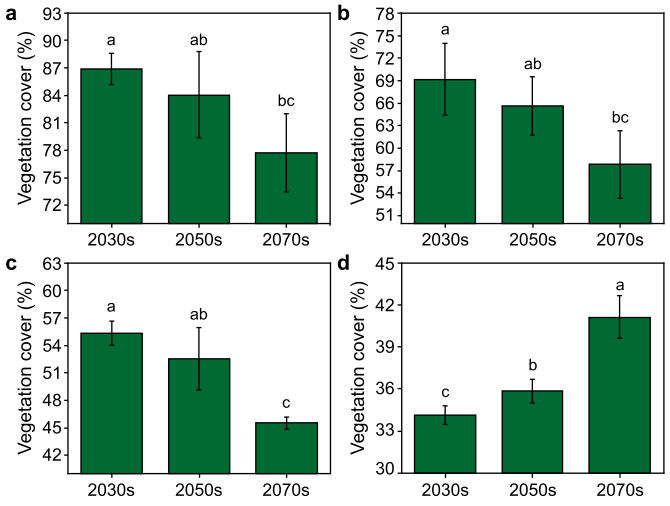

Fig. 6. Forecasted vegetation cover in the 2030s, 2050s, and 2070s within the four different vegetation zones (Fig. S1) of China's Loess Plateau. **a**, Temperate, semi-humid, broad-leaved, deciduous forest zone (TSFZ). **b**, Temperate arid forest zone (TAFZ). **c**, Temperate semi-arid steppe zone (TSSZ). **d**, Temperate arid steppe zone (TASZ). Each bar represents the forecasted cover averaged across the three emission scenarios. Bars with different letters are significantly different ($P < 0.05$).

increased rapidly in the last millennia, coincident with the steep decline in vegetation cover on the Loess Plateau (Fig. S3a) and accompanied by a rapid increase in sediment discharge (Fig. S3b). Previous research has suggested that the Yellow River Basin was relatively safe from flooding (frequency 2–14 floods per century) for the 2000 years spanning the Shang, Zhou, Qin, and Han Dynasties [35]. Since the late Tang Dynasty, flooding has increased from >50 to >100 times per century from the Ming Dynasty through the early days of the People's Republic of China [34]. The frequency of conflicts increased much more slowly in the same three millennia, from ~33 wars per century between 2070 BCE and 960 CE to ~55 wars per century in the subsequent 600 years. Increased flooding and sedimentation across the Loess Plateau are much more closely tied to vegetation change (through human land-use changes) than the frequency of conflicts (Fig. S3).

In the recent conflict-free decades, vegetation growth on the Loess Plateau has been closely associated with climatic factors (Fig. 7); vegetation cover has been significantly and positively correlated with rainfall and temperature but negatively correlated with evaporation, wind speed (Fig. 7, top), and sediment load in the Yellow River (Fig. S4). It is well known that ~90% of the sediment in the Yellow River derives from soils eroded from the Loess Plateau [40,41]; thus, the quantity of sediment in the Yellow River Basin is a strong indicator of vegetation changes on the Loess Plateau.

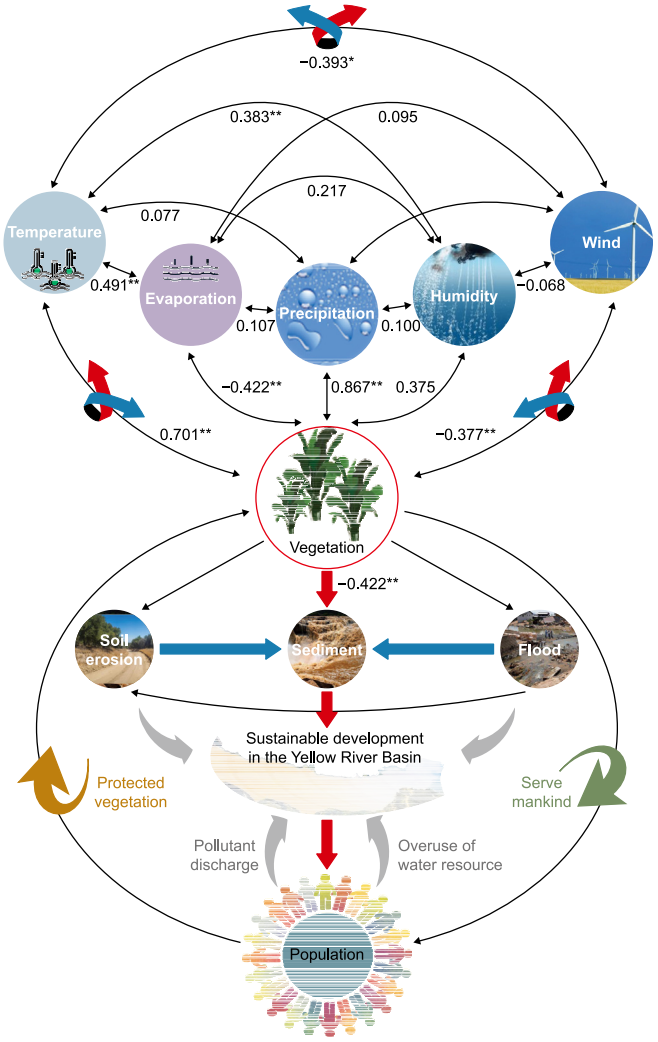

Fig. 7. Pairwise correlations and sustainable development in the Yellow River Basin. Top: Correlations among temperature, precipitation, humidity, wind speed, evaporation, and vegetation cover. Bottom: Potential implications of these correlations for sustainable development.

The GFG project has changed the landscape of the Loess Plateau [3,42], but ongoing climatic change will make it difficult to consolidate the achievements of the GFG project or to achieve sustainable development in the region. Climatic change is undeniable, and vegetation cover on the Loess Plateau is forecast to decrease with increases in CO_2 and temperature. As vegetation cover decreases, soil erosion and flood frequency likely will increase, each with strong negative effects on sustainable social and economic development in the Yellow River Basin (Fig. 7, bottom). The continuous increase in evaporation without concomitant increases in rainfall will exacerbate the trend to a warmer and drier climate.

The planting over large areas of vegetation that consume a lot of water leads to the formation of a dry soil layer and the gradual decline of the soil reservoir [43,44]. The average thickness of the dry soil layer in the Loess Plateau was 1.6 m, and the average thickness of the forest dry soil layer was 3.0 m [45]. In the semi-humid and semi-arid region of the Loess Plateau, the dry soil layer thickness of *Pinus tabulaeformis* plantations was up to 5.0 m, and that of *Robinia pseudoacacia* plantations was 4.9 m. Even in the semi-humid region, the dry soil layer thickness of *P. tabulaeformis* plantations was 3.9 m, and that of *R. pseudoacacia* plantations was 2.5 m [46]. Previous research has shown that the average vegetation carrying capacity of soil water resource on the Loess Plateau is 400 ± 5 g C m^{-2} yr^{-1}. The value is forecast to decline to 383 g C m^{-2} yr^{-1} under global warming conditions [47]. This observation suggests three directions for future management.

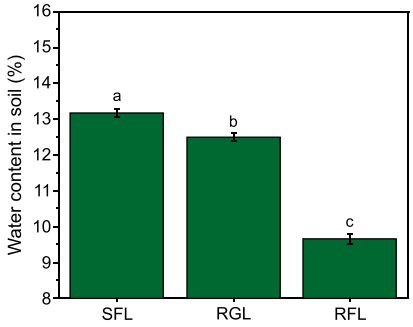

Fig. 8. Soil water content (mean ± S.E.) at 30 cm depth in the sloping farmland (SFL), returning farmland to grassland (RGL), and returning farmland to forestland (RFL). Differences among means at the three sites were compared using one-way ANOVA; different letters denote significant differences ($P < 0.05$; Tukey post-hoc test, $n = 6$).

First, if vegetation cover indeed has peaked on the Loess Plateau, especially in the southeast, further expansion of vegetation as part of the GFG project could be ecologically counterproductive. Therefore, returning the forestland to grassland would improve the sustainability of the Yellow River Basin. The soil water content at 30-cm depth was 21.63% lower in forestland than in grassland (Fig. 8). Second, planting herbaceous plants with shallow, dense, and fibrous roots on hillsides could reduce erosion more effectively than additional trees, which have deep, sparse, and straight roots. In contrast, trees and shrubs should be planted in ditch bottoms with abundant water. Third, enhanced water management is crucial for sustaining agricultural productivity on the Loess Plateau, where water scarcity limits plant growth and agricultural productivity. Although annual rainfall across the Loess Plateau is ~466 mm, it decreases from ~600 to 700 mm in the southeast to only 100–200 mm in the northwest. In addition, most rain falls between July and September in the gully region of the Loess Plateau and usually leads to severe flooding. We recommend integrating historical data with contemporary forecasts to design once-in-a-century reservoirs to reduce flooding following heavy rainfall. These reservoirs also could provide water for irrigation during periods of drought on the Loess Plateau [48].

4. Conclusion

Climatic warming has occurred worldwide, and the average rate of warming on the Loess Plateau was 0.27 °C per decade, more than double the global average (0.12 °C per decade). Such trends pose challenges to reinforcing the gains of the GFG project and to achieving sustainable development in the Yellow River Basin.

Over the past 70 years, vegetation has increased gradually, especially after implementing the GFG project. The vegetation cover was 53% in 2012, comparable to the historical maximum recorded during the Xia Dynasty. However, the vegetation cover has tended to decline since 2019 (64.98%), indicating that 53–65% is the sustainable threshold interval of vegetation on the Loess Plateau. The average vegetation cover on the Loess Plateau is 65%, 63%, and 62% in the 2030s, 2050s, and 2070s using species distribution models (SDMs) under low, intermediate, and high emission scenarios. From the observation data, the vegetation cover on the Loess Plateau reached a peak threshold value in 2019.

Vegetation cover exerts a direct impact on sediment discharge and sustainable development of the Yellow River Basin. Consequently, the quantity of sediment in the Yellow River Basin serve as a strong indicator of vegetation changes on the Loess Plateau. Therefore, adapting vegetation management strategies to climate change is imperative. First, the vegetation cover has a peak threshold value on the Loess Plateau, especially in the southeast, so further expansion under the GFG project risks ecological detriment. Second, planting herbaceous plants with shallow, dense, and fibrous roots on hillsides could reduce erosion more effectively than additional trees with deep, sparse, and straight roots. Third, improving water management is crucial for sustaining agricultural productivity on the Loess Plateau, where water scarcity constrains plant growth and agricultural productivity.

The study puts forward the vegetation coverage threshold for sustainability of ecological constructure on the Loess Plateau by analyzing vegetation changes from past, present and future, so as to provide scientific reference for ecological civilization construction and management in semi-humid and semi-arid region regions of the world.

CRediT authorship contribution statement

Yi-ping Chen: Data Curation, Funding Acquisition, Investigation, Methodology, Validation, Writing - Original Draft, Writing - Review & Editing. **Kai-bo Wang:** Investigation, Writing - Review & Editing. **Bo-jie Fu:** Conceptualization. **Yan-fen Wang:** Writing - Review & Editing. **Han-wen Tian:** Data Curation, Software, Visualization, Writing - Review & Editing. **Yi Wang:** Writing - Review & Editing. **Yi Zhang:** Writing - Review & Editing.

Declaration of competing interest

The authors declare that they have no known competing financial interests or personal relationships that could have appeared to influence the work reported in this paper.

Acknowledgments

The National Natural Science Foundation of China (42041005, U2243225) supports this research.

Appendix A. Supplementary data

Supplementary data to this article can be found online at https://doi.org/10.1016/j.ese.2024.100442.

References

[1] L. Deng, S. Liu, D.G. Kim, C. Peng, S. Sweeney, Z. Shangguan, Past and future carbon sequestration benefits of China's grain for green program, Global Environ. Change 47 (2017) 13–20.
[2] C.O. Delang, Z. Yuan, China's Grain for Green Program: A Review of the Largest Ecological Restoration and Rural Development Program in the World, Springer International Publishing, 2015.
[3] Y. Chen, K. Wang, Y. Lin, W. Shi, Y. Song, X. He, Balancing green and grain trade, Nat. Geosci. 10 (2015) 739–741.
[4] C. Chen, T. Park, X. Wang, S. Piao, B. Xu, R.K. Chaturvedi, R.B. Myneni, China and India lead in greening of the world through land-use management, Nat. Sustain. 2 (2019) 122–129.
[5] J. Bongaarts, Intergovernmental panel on climate change special report on global warming of 1.5°C, Switzerland: IPCC, 2018, Popul. Dev. Rev. 45 (2018) 251–252.
[6] T. Park, S. Ganguly, H. Tømmervik, E.S. Euskirchen, K.-A. Høgda, S.R. Karlsen, R.B. Myneni, Changes in growing season duration and productivity of northern vegetation inferred from long-term remote sensing data, Environ. Res. Lett. 11 (2016) 084001.
[7] J. Spinoni, P. Barbosa, E. Bucchignani, J. Cassano, T. Cavazos, J.H. Christensen, A. Dosio, Future global meteorological drought hotspots: a study based on CORDEX data, J. Clim. 33 (2019) 3635–3659.
[8] R.S. Padrón, L. Gudmundsson, B. Decharme, A. Ducharne, D.M. Lawrence, J. Mao, S.I. Seneviratne, Observed changes in dry-season water availability attributed to human-induced climate change, Nat. Geosci. 13 (2020) 477–481.
[9] P.D.A. Kraaijenbrink, E.E. Stigter, T. Yao, W.W. Immerzeel, Climate change decisive for Asia's snow meltwater supply, Nat. Clim. Change 11 (2021) 591–597.
[10] H.J. Fowler, S. Blenkinsop, C. Tebaldi, Linking climate change modelling to impacts studies: recent advances in downscaling techniques for hydrological modelling, Int. J. Climatol. 27 (2007) 1547–1578.
[11] Y. Sun, J. Chang, J. Fang, Above- and belowground net-primary productivity: a field-based global database of grasslands, Ecology 104 (2023) e3904, e3904.
[12] J.T. Thorson, J.N. Ianelli, E.A. Larsen, L. Ries, M.D. Scheuerell, C. Szuwalski, E.F. Zipkin, Joint dynamic species distribution models: a tool for community ordination and spatio-temporal monitoring, Global Ecol. Biogeogr. 25 (2016) 1144–1158.
[13] H. George, C. Louise, S. Ritvik, Harmonization of global land-use change and management for the period 850–2100 (LUH2) for CMIP6, Geosci. Model Dev. (GMD) 13 (2020) 5425–5464.
[14] Y. Wang, M. Shao, H. Shao, A preliminary investigation of the dynamic characteristics of dried soil layers on the Loess Plateau of China, J. Hydrol. 381 (2010) 9–17.
[15] V. Almpanidou, G. Schofield, A.S. Kallimanis, C. Graeme Mazaris, D. Antonios, Using climatic suitability thresholds to identify past, present and future population viability, Ecol. Indicat. 71 (2016) 551–556.
[16] B.A. Reutter, V. Helfer, A.H. Hirzel, P. Vogel, Modelling habitat-suitability using museum collections: an example with three sympatric Apodemus species from the Alps, J. Biogeogr. 30 (2003) 581–590.
[17] J. Gao, X. Mu, W. Sun, Spatiotemporal variation of vegetation coverage on the Loess Plateau during 1981-2012, Soil.Water.Conserv. 36 (2016) 52–56 (in Chinese).
[18] H.J. Qiu, M.M. Cao, Spatiotemporal variation of vegetation cover in China based on SPOT VEGETATION data, Resour. Sci. 33 (2011) 335–340.
[19] Y. Zhang, Z. Zhao, S. Li, X. Meng, Indicating variation of surface vegetation cover using SPOT NDVI in the northern part of North China, Geogr. Res. 27 (2008) 745–754.
[20] A.S. Hope, W.L. Boynton, D.A. Stow, Interannual growth dynamics of vegetation in the Kuparuk river watershed, Alaska based on the normalized difference vegetation index, Int. J. Rem. Sens. 24 (2003) 3413–3425.
[21] S. Liu, T. Wang, J. Guo, J. Qu, P. An, Vegetation change based on SPOT-VGT data from 1998 to 2007, northern China, Environ. Earth Sci. 60 (2010) 1459–1466.
[22] Y. Song, M. Ma, Study on vegetation cover change in northwest China based on SPOT VEGETATION data, J. Desert Res. 27 (2007) 89–93.
[23] Z. Wang, Z. Guo, K. Song, L. Luo, B. Zhang, D. Liu, N. Huang, C. Ren, Responses of vegetation NDVI to climate change in Northeast China, J. Chem. Ecol. 28 (2009) 1041–1048.
[24] J. Bai, J. Bai, L. Wang, Spatiotemporal variation of vegetation NDVI and its relationship with regional climate in northern Shaanxi province during 2000-2010, Geogr. Sci. 34 (2014) 882–888.
[25] D. Stow, S. Daeschner, A. Hope, D. Douglas, A. Petersen, R. Myneni, L. Zhou, W. Oechel, Variability of the seasonally integrated normalized difference vegetation index across the North slope of Alaska in the 1990s, Int. J. Rem. Sens. 24 (2003) 1111–1117.
[26] R.K. Pachauri, L.A. Meyer, IPCC, 2014: climate change 2014: synthesis report. Contribution of working groups I, II and III to the fifth assessment report of the intergovernmental panel on climate change, IPCC, Geneva, Switzerland (2014).
[27] H. Tian, L. Liu, Z. Zhang, H. Chen, X. Zhang, T. Wang, Z. Kang, Spatiotemporal differentiation and attribution of land surface temperature in China in 2001–2020, J. Geogr. Sci. 34 (2024) 375–396.
[28] S. Feng, Q. Fu, Expansion of global drylands under a warming climate, Atmos. Chem. Phys. 13 (2013) 10081–10094.
[29] G. Wu, N. Wang, S. Hu, L. Tian, J. Zhang, Physical Geography, Higher Education Press, Beijing, 2008.
[30] H. Zou, Graphs of Vegetation Regionalization on the Loess Plateau (2000),Data Sharing Infrastructure of Earth System Science_Data Sharing Infrastructure of Loess Plateau, 2013.
[31] R.J. Scholes, The future of semi-arid regions: a weak fabric unravels, Climate 8 (2020) 8030043.
[32] W. Shen, M. Li, C. Huang, T. He, X. Tao, A. Wei, Local land surface temperature change induced by afforestation based on satellite observations in Guangdong plantation forests in China, Agric. For. Meteorol. 276–277 (2019) 107641.
[33] R. Liu, L.L. Xiao, Z. Liu, J.C. Dai, Quantifying the relative impacts of climate and human activities on vegetation changes at the regional scale, Ecol. Indicat. 93 (2018) 91–99.
[34] Z. Li, F.L. Zheng, W.Z. Liu, D.J. Jiang, Spatially downscaling GCMs outputs to project changes in extreme precipitation and temperature events on the Loess Plateau of China during the 21st Century, Global Planet. Change 82–83 (2012) 65–73.
[35] Z. Li, F. Zheng, W. Liu, Spatiotemporal characteristics of reference evapotranspiration during 1961-2009 and its projected changes during 2011-2099 on the Loess Plateau of China, Agric. For. Meteorol. 154 (2011) 47–155.
[36] N. Shi, Study on the historical geography of the Loess Plateau, Yellow River Conservancy Press (2001).
[37] L. Wang, M. Shao, Q. Wang, W. Gale, Historical changes in the environment of the Chinese Loess Plateau, Environ. Sci. Pol. 9 (2006) 675–684.

[38] H.M. Pereira, P.W. Leadley, V. Proenca, R. Alkemade, J.P.W. Scharlemann, Fernandez-Manjarres, M. Walpole, Scenarios for global biodiversity in the 21st century, Science 330 (2010) 1496–1501.
[39] C. Parmesan, C. Duarte, E. Poloczanska, A.J. Richardson, M.C. Singer, COMMENTARY: overstretching attribution, Nat. Clim. Change 1 (2011) 2–4.
[40] Y. Yu, H. Wang, X. Shi, X. Ran, T. Cui, S. Qiao, Y. Liu, New discharge regime of the huanghe (Yellow River): causes and implications, Continent. Shelf Res. 69 (2013) 62–72.
[41] Z. Jin, Y. Dong, Y. Wang, X. Wei, Y. Wang, B. Cui, W. Zhou, Natural vegetation restoration is more beneficial to soil surface organic and inorganic carbon sequestration than tree plantation on the Loess Plateau of China, Sci. Total Environ. 485–486 (2014) 615–623.
[42] J. Wang, W. Zhao, G. Wang, S. Yang, P. Pereira, Effects of long-term afforestation and natural grassland recovery on soil properties and quality in Loess Plateau (China), Sci. Total Environ. 770 (2021) 144833.
[43] L. Deng, W. Yan, Y. Zhang, Z. Shang Guan, Severe depletion of soil moisture following land-use changes for ecological restoration: evidence from northern China,For, Ecol. Manag. 366 (2016) 1–10.
[44] B. Fu, S. Wang, Y. Liu, J. Liu, W. Liang, C. Miao, Hydrogeomorphic ecosystem responses to natural and anthropogenic changes in the Loess Plateau of China. Annu, rev. Earth planet, Sci. 45 (2017) 223–243.
[45] Y. Wang, M. Shao, H. Shao, A preliminary investigation of the dynamic characteristics of dried soil layers on the Loess Plateau of China, J. Hydrol. 381 (2010) 9–17.
[46] Y. Wang, M. Shao, Y. Zhu, Z. Liu, Impacts of land use and plant characteristics on dried soil layers in different climatic regions on the Loess Plateau of China, Agric. For. Meteorol. 151 (2011) 437–448.
[47] X. Feng, B. Fu, S. Piao, S. Wang, P. Ciais, Z. Zeng, B. Wu, Revegetation in China's Loess Plateau is approaching sustainable water resource limits, Nat. Clim. Change 6 (2016) 1019–1022.
[48] Y. Chen, Y. Zhang, Sustainable model of rural vitalization in hilly and gully region on Loess Plateau, Bull. Chin. Acad. Sci. 34 (2019) 708–716.